ACS OMEGA

http://pubs.acs.org/journal/acsodf

Article

Sulfonated Poly Ether Sulfone Membrane Reinforced with Bismuth-Based Organic and Inorganic Additives for Fuel Cells

Anie Shejoe Justin Jose Sheela, Siva Moorthy, Berlina Maria Mahimai, Karthikeyan Sekar, Dinakaran Kannaiyan, and Paradesi Deivanayagam*

Cite This: *ACS Omega* 2023, 8, 27510−27518

Read Online

ACCESS | Metrics & More | Article Recommendations | Supporting Information

ABSTRACT: This research work focuses on developing a robust polymer electrolyte membrane (PEM) with high proton efficiency toward proton exchange membrane fuel cells (PEMFCs). In this study, poly ether sulfone (PES) was sulfonated by chlorosulfonic acid to yield sulfonated poly ether sulfone (SPES) followed by incorporation with bismuth-based additives such as bismuth trimesic acid (BiTMA) and bismuth molybdenum oxide (Bi_2MoO_6). The composite membrane was thoroughly investigated for its structural and physicochemical properties such as FT-IR, SEM, TGA, contact angle, water uptake, oxidative stability, ion-exchange capacity, and swelling ratio. Incorporation of additives into the polymer was confirmed by XPS and XRD analysis. The proton conductance of the pristine SPES is 4.19 × 10^{-3} S cm^{-1}, whereas that of the composite membrane SPES/BiTMA-10 is 10 × 10^{-3} S cm^{-1} and that of SPES/Bi_2MoO_6-15 is 7.314 × 10^{-3} S cm^{-1}; both the composite membranes exhibit higher proton conductivity than the pristine SPES membrane. The physicochemical characteristics and impedance measurements of the electrolyte reported can be viable to the PEM membrane.

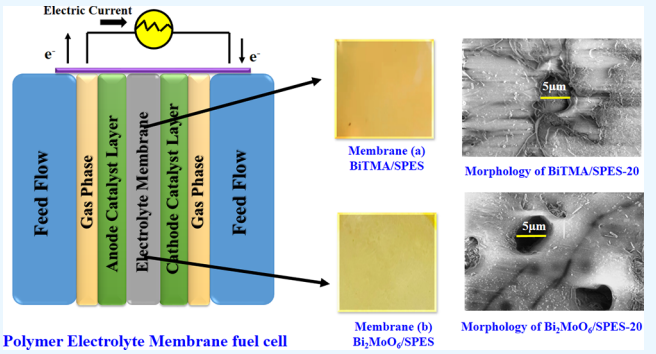

1. INTRODUCTION

Global development that continues to exist and has a direct impact on economic progress, industrial development, and human well-being is the lack of adequate access to clean energy sources. Fossil fuels, which historically have dominated the energy industry, are the main contributors to the emissions of carbon dioxide (CO_2) and other greenhouse gases, including petroleum fuels, natural gas, coal, and others.[1] Access to sustainable energy sources must be widely available for the development of new clean energy sources. Hence, energy storage systems like battery systems, redox flow batteries, and other fuel cell-based technologies should be effectively integrated side by side while enhancing their advanced features of renewable energy sources.[2]

British physicist Robert Grove developed the first fuel cell that used hydrogen and oxygen roughly 180 years ago, and several additional types of fuel cells were created in the 19th century after further research.[3] The polymer electrolyte membrane fuel cell (PEMFC) that further quickly turns the chemical energy of hydrogen into electricity has emerged as the most well-liked commercial fuel cell in recent years.[4] In a PEMFC, hydrogen gas, which has the highest energy density, and oxygen, which comes from the air, are used in a few electrochemical reactions on the surface of an electrode.[5] In the middle of a PEMFC, anode and cathode electrodes are combined with an electrolyte layer, and a conductive layer is positioned on each upper side of the cell. Low-temperature and high-temperature PEMFCs are two significant subtypes of PEM fuel cells.[6] PEMs use hydrogen as a fuel and polymer membrane as an electrolyte. It gained considerable popularity due to its numerous advantages, such as high density of power, elevated efficiency in converting energy, and fast start with low environmental impact.[7]

For the past few decades, there are many developments and alternations for the perfluorosulfonic acid polymer electrolyte membrane, i.e., Nafion, because of its huge advantages like strong C−F bonds attached with sulfonic acid as its end group in the hydrophobic backbone and high mechanical and thermal stability. Even though Nafion displays very good proton conductivity and good mechanical stability, it has many disadvantages also such as water flooding, high oxygen permeability, poor thermal stability, dehydration at $T > 80$ °C, and high cost.[8] The essential requirements of PEMFC include the following: (i) the electrolyte membrane should be mechanically and thermally stable, (ii) the change in

Received: May 7, 2023
Accepted: June 21, 2023
Published: July 22, 2023

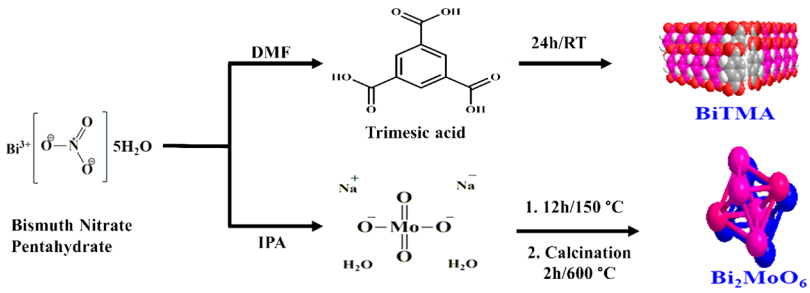

Figure 1. Preparation of Bi_2MoO_6 and BiTMA.

membrane area between the dry and swollen states should be negligible, (iii) the proton conductivity of the membrane should be high, (iv) the thickness of the membrane should be less to minimize the resistance, and (v) the membrane/electrode interface resistance should be minimized.[9−12] Hence, we need an alternate polymer membrane for the PEMFC. There is much ongoing research to find a good alternative for Nafion like poly (ether ether sulfone),[13] poly (ether ether ketone),[14] poly (vinyl alcohol),[15] polyimides,[16] poly (benzimidazole),[17] porous organic polymers,[18] etc.

To sort out these provocations, in our research, we have used an aromatic hydrocarbon-based polymer network like poly ether sulfone (PES). PES is a high-performance thermoplastic polymer with amorphous, translucent, high resistance, and pale amber color characteristics. It has high water absorption rate and is sensitive to minor amounts of moisture in the air, causing dimensional alterations. It has excellent resistance to aliphatic hydrocarbons, chlorinated hydrocarbons, and aromatics with ease. It exhibits excellent mechanical stability, is cost-efficient, and has film-forming capacity. The sulfonation process gives the parent aromatic polymer several desirable properties, including greater ionic conductivity, better hydrophilicity, and higher solubility. Sulfonating PES provides improved proton transport, which is essential for high proton conduction in fuel cells. Furthermore, the addition of sulfonic acid groups turns the parent polymer into ionomers without damaging the polymer chain and raises the glass transition temperature. Controlling sulfonation allows you to adjust the number of sulfonic acid groups in your product, also known as sulfonation degree (DS).[19] SPES/MNFs, a unique flower-like MIL-53(Al)-NH_2 nanofiber-blended proton exchange membrane, were reported by Wang *et al.* The composite membrane demonstrated a remarkable improvement in proton conductivity up to 0.201 S cm^{-1} as the MNF content is high up to 5 wt %, attaining a simultaneous improvement in membrane stability and proton conduction.[20]

For the PEM membrane, there is an addition of fillers that increase the IEC, water uptake, and proton conductivity. The fillers can be organic, inorganic, and carbon nanomaterials that have hydrolytic stability. Dual metal oxides have been proposed as a potential alternative to generate greater electroactivity. High catalytic activity and a strong interfacial active band are found in dual metal oxides. Furthermore, using dual metal oxides as a filler in polymers will improve durability and allow for homogeneous dispersion.[21] Bi_2MoO_6 is a dual metal oxide that can hold a lot of oxygen and has a strong interaction between metals. It also has high electrical conductivity, stability in catalysis, and resistance to corrosion.[22] Studies of porous metal−organic frameworks (MOFs) and polymers that are combined to generate PEMs have garnered a lot of attention recently. MOFs can be made when metal ions or clusters and organic ligands come together on their own.[23] Metal−organic frameworks (MOFs) with high proton conductivity have gotten a lot of interest recently. Protons were discovered to be transported through the coordinating skeleton or carriers. In addition, MOF has a large specific surface area, and it can hold more proton carriers, which opens the door to increasing the composite membrane's proton conductivity. Improved selectivity can be achieved by preventing fuel and oxidant from diffusing through MOF's narrow pore size.[24] The interaction zone is created by the dispersion of nanofillers into the polymer matrix, which enhances the membrane properties. The hydrogen bonding interaction formed between SPES and the bismuth nanofiller improves the performance and stability of the prepared composite membranes.[25−27] Furthermore, due to their unique and different crystal structures, directly processing MOFs for fuel cells is extremely difficult.[28] BiTMA is an organic hybrid material with a unique crystal structure. The open framework structure of MOFs was discovered to increase the composite membrane's performance by loading particles with particular functions into the matrix as proton carriers.[29,30] MOFs have a large specific surface area, which permits the composite membrane to facilitate proton migration while supporting more bound water, improving proton hopping conductivity even more. Furthermore, the small pore size in MOF can obstruct fuel and oxidant diffusion, lowering selectivity, and most MOFs contain multiple proton hopping sites, which can raise conductivity.

Herein, we have reported the composite membranes prepared from the bismuth-based metal−organic framework and dual metal oxides based on bismuth and molybdenum with sulfonated poly ether sulfone. The developed membranes were characterized by FT-IR, XRD, SEM, XPS, TGA, and physicochemical characterization like water uptake, IEC, and contact angle. The comparison studies were performed for MOF- and dual metal oxide-based polymer composites. Moreover, both types of composites exhibit good results, but the dual metal oxides seem to be the potential additive for SPES polymer to operate in the PEMFC.

2. EXPERIMENTAL SECTION

2.1. Materials. Poly ether sulfone (PES) was gifted by Garda Chemicals Ltd., Mumbai. Concentrated sulfuric acid and trimesic acid (H_3BTC) were purchased from Sigma-Aldrich. *N*-Methyl 2-pyrrolidine (NMP), dimelthylformamide, chlorosulfonic acid, bismuth(III) nitrate pentahydrate ($Bi(NO_3)_3{\cdot}5H_2O$) were procured from SRL. Methanol, sodium hydroxide, isopropyl alcohol, and sodium molybdate dihydrate

https://doi.org/10.1021/acsomega.3c03143
ACS Omega 2023, 8, 27510−27518

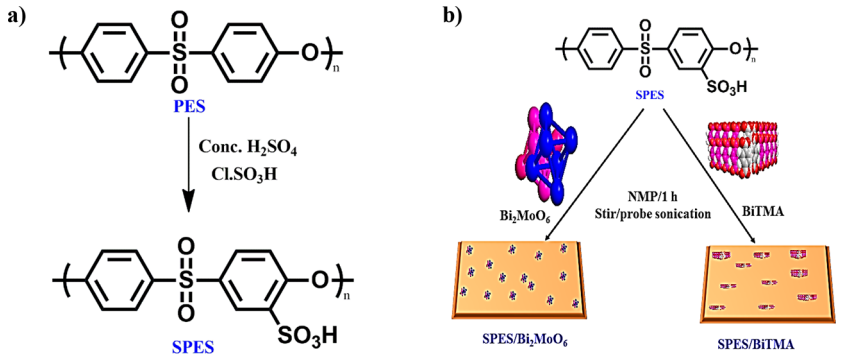

Figure 2. Scheme for the preparation of (a) SPES and (b) polymer composite membranes.

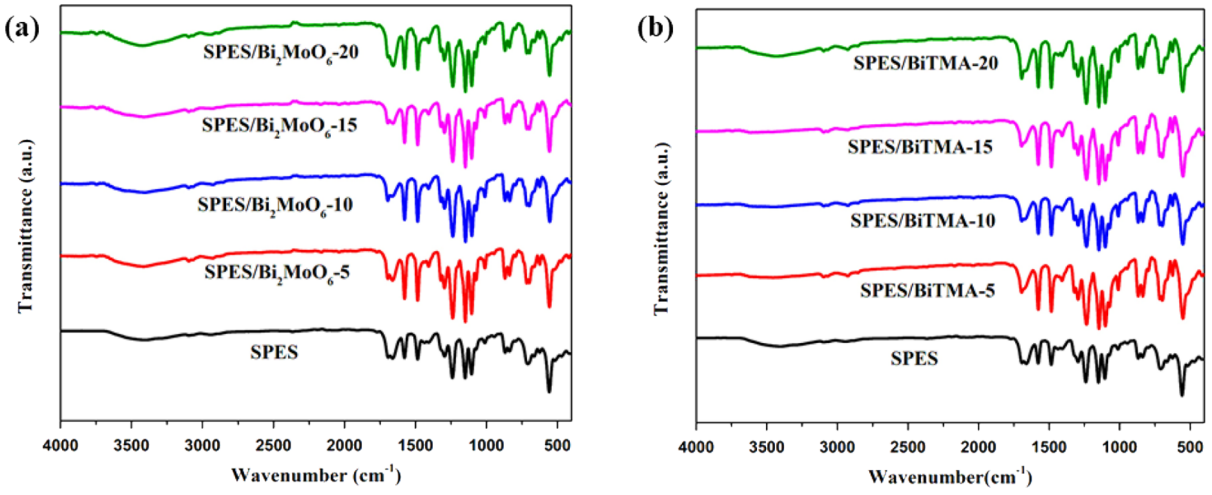

Figure 3. FT-IR spectra of (a) $SPES/Bi_2MoO_6$ and (b) BiTMA samples.

($Na_2MoO_4{\cdot}2H_2O$) were purchased from Qualigens and used as received.

2.2. Synthesis of Bi-MOF. The bismuth metal−organic framework was synthesized by a co-precipitation process.[32] In this method, 0.98 mmol of $Bi(NO_3)_3{\cdot}5H_2O$ and 1.84 mmol of H_3BTC were dissolved in 20 mL of DMF/methanol solvent mixture (1:3) slowly under constant stirring for 24 h. The obtained solution was centrifuged at 2000 rpm for 10 min. The resulting white precipitate was washed again and again with methanol and DI water. The precipitate (BiTMA) was dried out in a hot-air oven at 80 °C for 24 h after centrifugation.

2.3. Synthesis of Dual Metal Oxide. The dual metal oxide was synthesized by a facile hydrothermal method.[33] The precursors 0.1 M $Bi(NO_3)_3{\cdot}5H_2O$ and 0.1 M $Na_2MoO_4{\cdot}2H_2O$ were dissolved in 20 mL of 1:1 ratio of water and isopropyl alcohol separately. Then, the $Na_2MoO_4{\cdot}2H_2O$ solution was added dropwise into $Bi(NO_3)_3{\cdot}5H_2O$ solution under vigorous stirring for 1 h and sonicated for 30 min. Finally, the reaction was carried out for 12 h at 150 °C in a Teflon-lined autoclave. Ethanol and water were used to centrifuge, filter, and wash the resultant mixture. The resulting precipitate was dried in the oven overnight at 80 °C. Then, the dried powder was calcined in a muffle furnace for 2 h at 600 °C. The resulted dual metal oxide (Bi_2MoO_6) powder was obtained in yellow color. Figure 1 shows the scheme for the preparation of Bi_2MoO_6 and BiTMA.

2.4. Synthesis of Sulfonated PES. The sulfonation of PES was carried out from the reported procedure.[31] PES pellets were initially dried at 120 °C for 2 h to reduce moisture content. A volume of 25 mL of con. H_2SO_4 was taken in a three-necked round-bottom flask, and the dried PES pellets (5 g) were added slowly in the reaction flask under constant stirring. After 20 min, 2.5 mL of chlorosulfonic acid was added drop by drop to the reaction medium under cool conditions. When the solution became completely homogeneous, the reaction was stopped and the mixture was quenched in ice-cold water. The obtained white beads of SPES polymer were washed with DI water until it reached neutral pH. To eliminate extra moisture, the beads were dried at 80 °C for 24 h in a hot-air oven. The dried polymer beads were stored in a vacuum desiccator and used for further studies. Figures S1 and S2 present the GPC chromatograms of PES and SPES polymer, respectively. The molecular weight of PES was found to be 53,066 g/mol. The weight average molecular weight (M_w) and polydispersity index (PDI) of SPES polymer were found to be 64,781 g/mol and 1.709, respectively.

2.5. Preparation of Polymer Composite Membranes. A solution casting method was used to prepare the polymer composite membranes. The polymer SPES dissolved with NMP at room temperature. Known amounts of MOF and dual metal oxide (5, 10, 15, and 20% by weight) were added to the viscous polymer solution, which was then thoroughly agitated for 1 h at room temperature. The solution was then cast onto a Petri dish, and the solvent was evaporated at 80 °C in an oven. The membrane was immersed in deionized water to peel it from the Petri dish, dried, and used for further characterization. The composite membranes were represented as SPES/Bi_2MoO_6-X wt % and SPES/BiTMA-X wt % (X = 5, 10, 15,

https://doi.org/10.1021/acsomega.3c03143
ACS Omega 2023, 8, 27510−27518

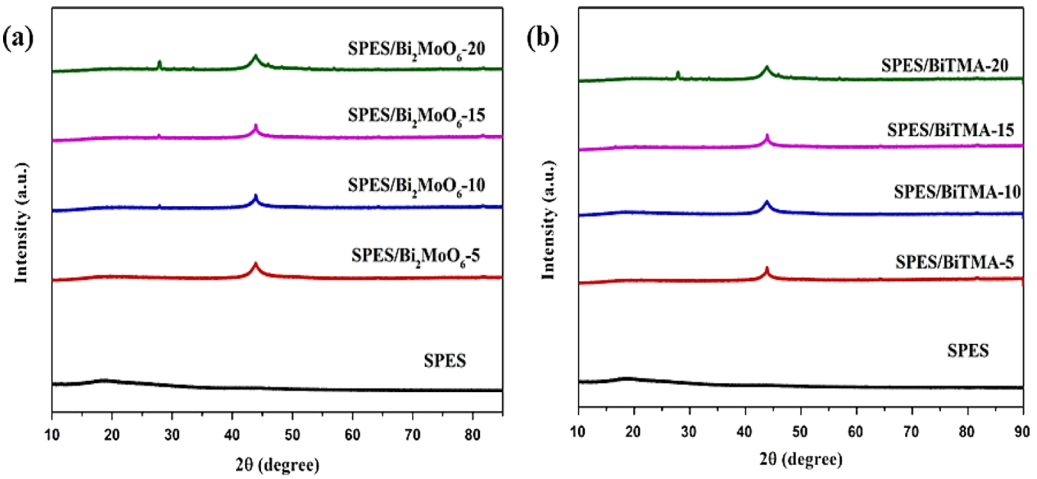

Figure 4. XRD patterns of (a) SPES and SPES/Bi_2MoO_6 and (b) SPES and SPES/BiTMA membranes.

and 20 wt %). The scheme for the synthesis of sulfonated PES and preparation of the composite membrane is depicted in Figure 2a,b. The prepared composite membranes were thoroughly examined in terms of structural, physical, and chemical properties. The characterization techniques and procedures are provided in the Supporting Information.

3. RESULTS AND DISCUSSION

3.1. Spectral Studies. The FT-IR spectra of Bi_2MoO_6 and BiTMA are displayed in Figure S3. The FT-IR peak appeared around 709 cm^{-1}, which was associated with the C−H bond in SPES. The presence of a peak at 1101 cm^{-1} indicated PES sulfonation. A signal at 1013 cm^{-1} indicated the symmetrical stretching vibration of sulfonic acid in the SPES polymer. The peak observed at 1493 cm^{-1} validates the benzene ring's stretching vibration. The large peak seen at 3425 cm^{-1} indicates the presence of hydroxyl group stretching vibration in the sulfonic acid-bound polymer. The peak at 459 cm^{-1} within the spectra of Bi_2MoO_6 dual metal oxide corresponds to such stretching and bending vibrations of bismuth oxide, while the peaks at 637 and 527 cm^{-1} correspond to stretching and bending vibrations of molybdenum oxide. The signal at 830 cm^{-1} is attributed to a Mo−O bond dual metal oxide, while the peak at 912 cm^{-1} indicates a stretching vibration of the Mo−O bond.[34] According to the spectra for BiTMA MOF, its peaks at 432 and 545 cm^{-1} correspond to the vibrational stretching of bismuth and oxygen, respectively. The signal at 935 cm^{-1} corroborates an O−H bond of trimesic acid.[35] The comparable frequency reported for Bi_2MoO_6 and BiTMA within the composite membrane validates the inclusion of Bi_2MoO_6 and BiTMA into SPES and validates the appearance of compounds in the polymer membrane. The FT-IR signal of each polymeric membrane of a double oxide and MOF is depicted in Figure 3.

3.2. XRD Analysis. XRD patterns of dual metal oxide and MOF are displayed in Figure S4. The sharp peaks that appeared at 28°, 33°, and 47° represent the crystal planes (111), (060), and (202), respectively,[36] which confirm the crystal structure of Bi_2MoO_6. The BiTMA MOF sample is also found to be crystalline in nature and confirmed by the major 2θ peaks at 23°, 28°, and 45°, which represent the crystal planes (003), (012), and (015),[37] respectively. From Figure 4a,b, the SPES polymer shows a broad peak at 20° and it confirms the amorphous nature of sulfonated PES. The crystallinity behavior was enhanced in the SPES polymer, which is due to the addition of Bi_2MoO_6 and BiTMA. From the XRD data, it is confirmed that the composite membranes are both amorphous and crystalline in nature.

3.3. Morphology Studies. The surface morphology of the prepared SPES, Bi_2MoO_6, BiTMA, SPES/Bi_2MoO_6-5, and SPES/BiTMA-20 composite membranes was investigated, and the images are displayed in Figure 5. The morphology of the

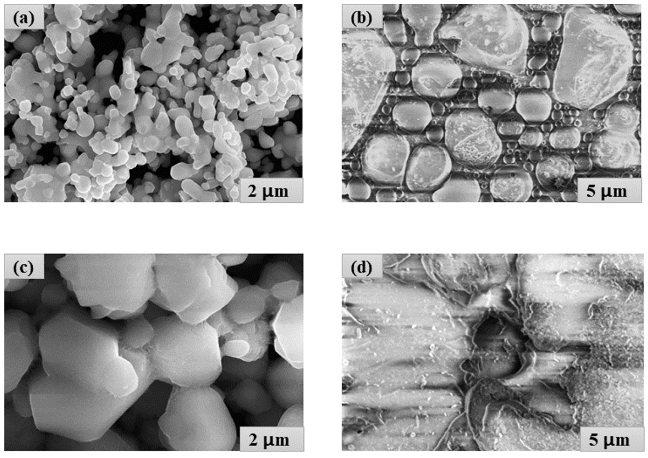

Figure 5. SEM views of the samples: (a) Bi_2MoO_6, (b) SPES/Bi_2MoO_6-5, (c) BiTMA, and (d) SPES/BiTMA-20.

pristine SPES sample shows a smooth surface with some voids due to the absorbance of solvent on the membrane surface. Both the prepared Bi_2MoO_6 dual metal oxide and BiTMA MOF are cuboid in structure (Figure 5a,c). The composite membranes (Figure 5b,d) of SPES/Bi_2MoO_6-5 and SPES/BiTMA-20 show pores on the surface of the polymer, which may be the hydrophilic segments that enhance the proton conduction pathway.[38]

3.4. XPS Analysis. XPS analysis was used to investigate the surface features of the composite membrane. Figure 6a shows that the sample's high-resolution C1s spectra revealed four distinct peaks with binding energies of 284.4, 285.1, 286.3, and 288.2 eV, which are assigned to C−C, C−S, C═O, and C═C, respectively. Figure 6b displays an O1s spectrum with a single peak at 529.9 eV for O═C. Figure 6c shows the S2p spectrum with intense peaks at 167.7, 164.6, and 159.2 eV, which confirms the sulfonation in the polymer backbone and the

https://doi.org/10.1021/acsomega.3c03143
ACS Omega 2023, 8, 27510−27518

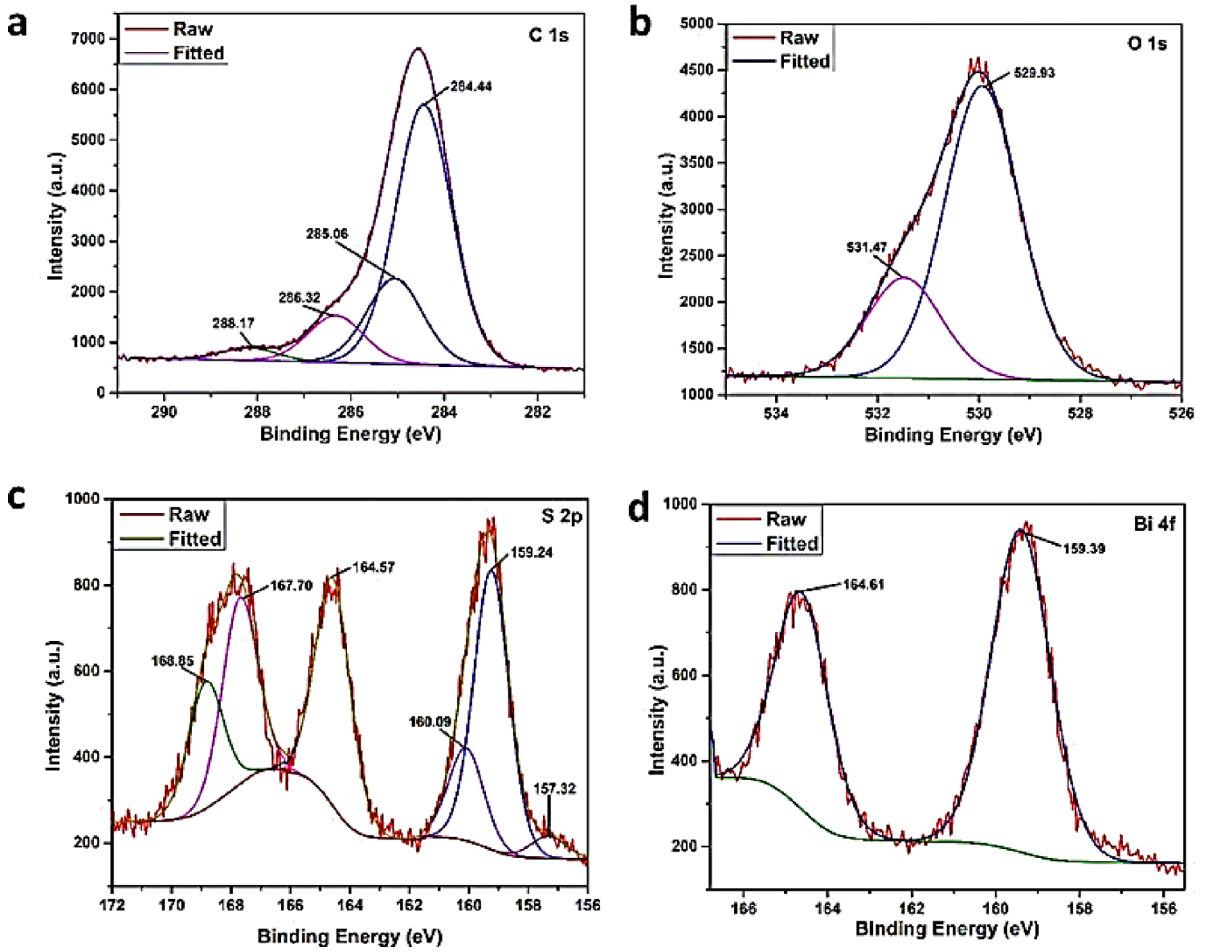

Figure 6. XPS data of the SPES/BiTMA-20 membrane: (a) carbon spectrum, (b) oxygen spectrum, (c) sulfur spectrum, and (d) bismuth spectrum.

presence of the sulfone group. The Bi4f spectrum is shown in Figure 6d, with two prominent peaks at 164.6 and 159.4 eV, indicating the f-orbital splitting energy levels of $Bi^{3+}4f_{5/2}$ and $Bi^{3+}4f_{7/2}$, respectively.[39]

Figure 7a shows the overall XPS data for the SPES/Bi_2MoO_6-20 membrane. Figure 7b shows that the sample's high-resolution C1s spectra revealed four distinct peaks with binding energies of 284.5, 285.7, 286.7, and 287.9 eV, which are assigned to C−C, C−S, C═O, and C═C, respectively. Figure 7c displays an O1s spectrum with a single peak at 531.8 eV for O−Mo. Figure 7d shows the S2p spectrum with intense peaks at 159.2, 164.5, and 168.3 eV, which prove the sulfonation in the polymer backbone and the presence of the sulfone group. The Bi4f spectrum is shown in Figure 7e, with two prominent peaks at 164.5 and 159.2 eV, indicating the f-orbital splitting energy levels of $Bi^{3+}4f_{5/2}$ and $Bi^{3+}4f_{7/2}$, respectively.[32] The Mo3d spectrum is shown in Figure 7f, with two prominent peaks at 232.1 and 235.3 eV, indicating the d-orbital splitting energy levels of $Mo^{6+}3d_{5/2}$ and $Mo^{6+}3d_{3/2}$, respectively.[40]

3.5. Thermogravimetric Analysis. The TGA curves of Bi_2MoO_6, BiTMA, SPES, SPES/Bi_2MoO_6-20, and SPES/BiTMA-20 composites are presented in Figure 8. The weight loss that appeared at 90−120 °C in the entire materials is due to the presence of bound water molecules. There is no degradation up to 650 °C for the prepared Bi_2MoO_6, which indicates that the materials are thermally more stable. The prepared BiTMA MOF shows the major degradation at 380 °C, which is due to the presence of organic linkers. SPES and hybrid membranes (SPES/BiTMA and SPES/Bi_2MoO_6) undergo three-step deterioration. The initial weight loss recorded up to 150 °C was due to the evaporation of solvent and water.[41] The second weight loss was attributed to the aromatic sulfonyl group in the backbone of the polymer at 280 °C. Due to the polymer chain degradation at 520 °C, its full weight loss was observed.

3.6. Contact Angle Measurements. By contact angle calculations, the equivalent hydrophilic nature and hydrophobicity of a prepared PEM can be assessed. The contact angles of SPES, SPES/Bi_2MoO_6-20, and SPES/BiTMA-20 are depicted in Figure S5. In general, the more hydrophilic sample demonstrates the lowest contact angle, which provides better proton conduction. The SPES and composite membranes of both dual metal oxide samples and MOF-based samples are hydrophilic in nature,[42] which shows good agreement to operate in PEMFC.

3.7. Physicochemical Properties of SPES and Composites. Water uptake, a fundamental characteristic for assessing a PEM's effectiveness in proton conduction, is principally influenced by the membrane's microstructure (porous structure) and functional groups in polymer rings. The amount of water is taken on a mass basis, which is determined by the quantity of water held within the membrane's pores and, thus, the interactions among molecules of water as well as the polar

https://doi.org/10.1021/acsomega.3c03143
ACS Omega 2023, 8, 27510−27518

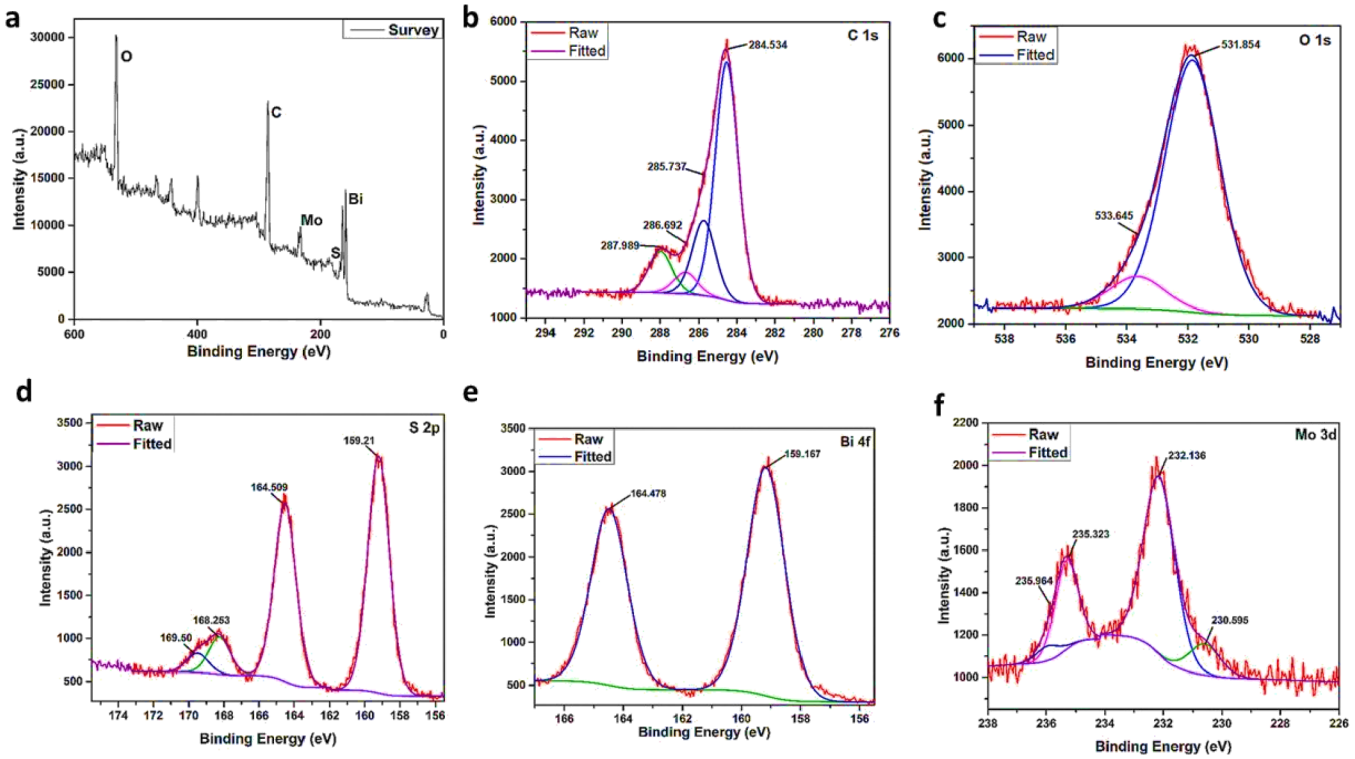

Figure 7. XPS data of the SPES/Bi_2MoO_6-20 membrane: (a) survey spectrum, (b) carbon spectrum, (c) oxygen spectrum, (d) sulfur spectrum, (e) bismuth spectrum, and (f) molybdenum spectrum.

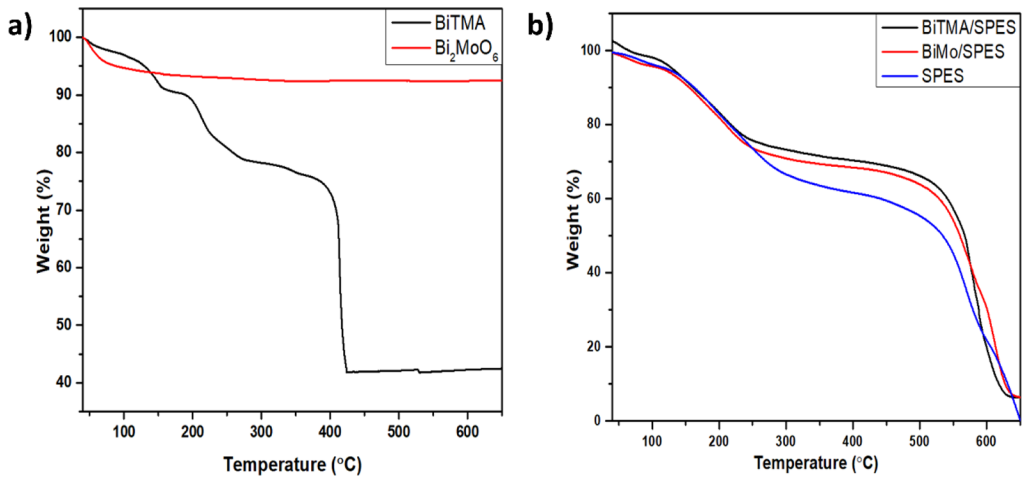

Figure 8. TGA analysis of (a) Bi_2MoO_6 and BiTMA and (b) SPES-pristine, SPES/Bi_2MoO_6-20, and SPES/BiTMA samples.

functional groups of the polymer.[43] The increased water absorption capacity is due to the sulfonic acid groups in the polymer backbone. The water uptake of pristine and composite membranes is represented in Table 1. The water uptake values were dropped as SPES/Bi_2MoO_6-20 > SPES/Bi_2MoO_6-15 > SPES/Bi_2MoO_6-10 > SPES/Bi_2MoO_6-5. Hence, the quantity of sulfonic acid groups effects the water intake directly.[44] The water uptake has been gradually increased as the loading of additives increases in SPES/Bi_2MoO_6 composite membranes. The SPES/Bi_2MoO_6-20 membrane exhibits the highest water absorption rate of all membranes. The addition of BiTMA to SPES reduces the membrane's water absorption compared to SPES/Bi_2MoO_6. Even as the miscibility between hydrophilic BiTMA and hydrophobic SPES has a large effect on lowering water uptake, the water uptake can be reduced.[42]

The swelling ratio is the fractional increase in the membrane dimension owing to water absorption. The swelling ratio was calculated using the difference in the length and thickness of the wet and dry membrane samples before and after water immersion. Excessive water uptake, on the other hand, would cause the membrane to bulge and lose its mechanical stability. For a membrane to function for an extended period of time in such a fuel cell application, it must be able to retain water and swell.[37] The values of the swelling ratio of SPES and composites are shown in Table 1. The swelling ratio decreases as the amount of Bi_2MoO_6 loaded increases. Incorporating MOF into the SPES polymer matrix causes more swelling.

IEC is the total active sites or functional groups in a PEM that are responsible for ion exchange. Significantly, the membrane IEC seems proportional to the quantity of sulfonic

https://doi.org/10.1021/acsomega.3c03143
ACS Omega 2023, 8, 27510−27518

Table 1. SPES and Composite Membranes' Physical and Chemical Properties

polymer code	ion exchange capacity[a] (meq g^{-1})	activation energy $\times 10^3$ (kJ mol^{-1})	oxidative stability[b] (%) at 80 °C	proton conductivity[c] $\times 10^{-3}$ (S cm^{-1})	water uptake[d] (%)	swelling ratio[e] (%)
SPES	1.81	13.85	81.66	4.19	8.14	2.38
SPES/BiTMA-5	1.56	11.81	89.03	9.02	10.34	4.52
SPES/BiTMA-10	1.30	17.40	95.16	10.00	10.58	4.76
SPES/BiTMA-15	1.60	11.98	92.65	8.61	11.33	5.26
SPES/BiTMA-20	2.03	14.72	92.83	2.97	12.89	5.53
SPES/Bi_2MoO_6-5	1.82	15.09	90.00	2.50	12.11	4.74
SPES/Bi_2MoO_6-10	1.70	13.50	87.34	4.27	14.96	5.00
SPES/Bi_2MoO_6-15	1.94	12.39	76.72	7.31	16.08	5.26
SPES/Bi_2MoO_6-20	2.22	14.63	65.71	3.02	20.01	5.41
Nafion 1100[46]	0.91	-	-	12.00	23.00	-

[a]IEC values are observed to be within ±0.065 meq g^{-1}. [b]Oxidative stability exhibits a variation of ±0.5%. [c]Proton conductivity shows a variation of ±0.001 S cm^{-1}. [d]Water uptake sweeps between ±0.75%. [e]Swelling ratio varies between ±0.60%.

acid that has been substituted in it. In general, the conductivities and water uptake of a membrane were directly related to its sulfonic acid group content.[45] Table 1 shows the measured IEC values of the pristine and composite membranes, wherein the SPES/Bi_2MoO_6 membrane found in the range between 1.8 and 2.2 meq g^{-1} shows an improvement in the IEC than the other membrane. The IEC of the SPES/BiTMA composites was found to be in the range between 1.5 and 2.0 meq g^{-1}. The degree of sulfonation (DS) of the SPES polymer was found to be 52.9%.

PEM's oxidative stability is critical, and it must be high to achieve long-term durability during fuel cell operation. The oxidative stability of PEM can be measured in situ and ex situ with Fenton's test, indicating ex situ durability.[45] The membrane's oxidative stability was assessed by immersing the polymer membrane in Fenton's solution at 80 °C, and the values are presented in Table 1. A dual metal oxide with lower concentration exhibited higher stability (90%) than the composite membrane loaded with a higher concentration of metal oxide, whereas increasing the concentration of MOF increases the oxidative stability, which is found to be 89 to 95% for the BiTMA-based composite membranes. Both Bi_2MoO_6 and BiTMA composite membranes possess good oxidative stability than the pristine SPES polymer, which contributes to their good durability and aids in proton conductivity enhancement.

3.8. Proton Conductivity and Activation Energy. Proton conductivity is a necessary characteristic of PEM that has a direct impact on the performance of fuel cells. Four-probe electrochemical impedance spectroscopy (EIS) is a widely used method for determining proton conductivity. In the vehicular mechanism, protons move with water as hydronium ions; however, in the Grotthuss mechanism, protons move by forming hydrogen bonds with water molecules.[47] The number of sulfonic acid groups influences the level of hydration, which has a substantial impact on the morphology (separation of hydrophilic and hydrophobic parts) of SPES membranes.[48] The proton conductivity measurements of the polymer composite membranes are depicted in Table 1. The ionic conductivity of the composite membrane SPES/BiTMA was found to be higher than that of the SPES/Bi_2MoO_6 membrane. The composite membranes derived from SPES/BiTMA-10 exhibit the highest proton conductivity of 10×10^{-3} S cm^{-1}. The pristine SPES polymer shows a value of 4.19×10^{-3} S cm^{-1}, which was lower than both the composite membranes. The MOF composite shows way less conductance than dual metal oxide.

Activation energy was calculated for pristine SPES and composite membranes. The activation energy of the SPES/Bi_2MoO_6-15 composite was found to be 12.393×10^3 kJ/mol, and that of SPES/BiTMA-15 was found to be 11.978×10^3 kJ/mol. The virgin SPES polymer showed a higher activation energy of 13.848×10^3 kJ/mol. The lower values of E_a of the composite indicate the presence of good proton conduction pathways.

4. CONCLUSIONS

Using sulfuric acid and chlorosulfonic acid, aromatic polyether sulfone was sulfonated. The two fillers, Bi_2MoO_6 and BiTMA, were synthesized by in-house methods. The additives bismuth molybdenum oxide and bismuth trimesic acid were embedded into SPES in four different concentrations. The solution casting procedure was used to construct all of the electrolyte membranes. FT-IR, XRD, contact angle, SEM, and XPS were used to confirm the structural investigation of composite membranes. Physicochemical characteristics including oxidative stability, water absorption, and IEC were carefully investigated. The composite membrane loaded with Bi_2MoO_6 shows good results than the pristine and SPES/BiTMA membranes. Both the composite membranes exhibit excellent thermal stability. Contact angle measurements reveal that the SPES/Bi_2MoO_6 and SPES/BiTMA composites were more hydrophilic than the SPES polymer. The highest proton conductivity (10×10^{-3} S/cm) was achieved for the composite membrane SPES/BiTMA-10. The SPES/Bi_2MoO_6-15 membrane displayed the ionic conductivity of 7.31×10^{-3} S/cm. From the overall studies, it is evidently confirmed that MOF-based SPES/BiTMA composites deliver good properties and are hence viable materials to operate in fuel cells.

■ ASSOCIATED CONTENT

Supporting Information

The Supporting Information is available free of charge at https://pubs.acs.org/doi/10.1021/acsomega.3c03143.

Materials characterization -GPC chromatogram of PES and SPES, FT-IR spectra of SPES, Bi_2MoO_6, and BiTMA samples -XRD pattern of Bi_2MoO_6 and BiTMA -contact angle images of neat SPES, SPES/Bi_2MoO_6-20, and SPES/BiTMA-5 composite membranes (PDF)

https://doi.org/10.1021/acsomega.3c03143
ACS Omega 2023, 8, 27510−27518

AUTHOR INFORMATION

Corresponding Author

Paradesi Deivanayagam − *Department of Chemistry, Faculty of Engineering and Technology, SRM Institute of Science and Technology, Kattankulathur 603203 Tamilnadu, India;* orcid.org/0000-0003-2894-0478; Email: paradesi77@yahoo.com

Authors

Anie Shejoe Justin Jose Sheela − *Department of Chemistry, Faculty of Engineering and Technology, SRM Institute of Science and Technology, Kattankulathur 603203 Tamilnadu, India*

Siva Moorthy − *Department of Physics and Nanotechnology, Faculty of Engineering and Technology, SRM Institute of Science and Technology, Kattankulathur 603203 Tamilnadu, India*

Berlina Maria Mahimai − *Department of Chemistry, Faculty of Engineering and Technology, SRM Institute of Science and Technology, Kattankulathur 603203 Tamilnadu, India*

Karthikeyan Sekar − *Department of Chemistry, Faculty of Engineering and Technology, SRM Institute of Science and Technology, Kattankulathur 603203 Tamilnadu, India*

Dinakaran Kannaiyan − *Department of Chemistry, Thiruvalluvar University, Vellore 632115 Tamilnadu, India*

Complete contact information is available at: https://pubs.acs.org/10.1021/acsomega.3c03143

Notes

The authors declare no competing financial interest.

ACKNOWLEDGMENTS

The authors wish to acknowledge Department of Chemistry, SRM Institute of Science and Technology (SRMIST), for providing gel permeation chromatography measurements. The authors sincerely acknowledge Nanotechnology Research Centre (NRC), SRMIST, Kattankulathur, Chengalpattu District, Tamilnadu, for providing the XPS facility to characterize the composite membranes.

REFERENCES

(1) Thomas, J. M.; Edwards, P. P.; Dobson, P. J.; Owen, G. P. Decarbonising energy: The developing international activity in hydrogen technologies and fuel cells. *J. Energy Chem.* **2020**, *51*, 405−415.

(2) Hou, J.; Yang, M.; Wang, D.; Zhang, J. Fundamentals and Challenges of Lithium Ion Batteries at Temperatures between −40 and 60 °C. *Adv. Energy Mater.* **2020**, *10*, 1904152.

(3) Karimi, M. B.; Mohammadi, F.; Hooshyari, K. Non-humidified fuel cells using a deep eutectic solvent (DES) as the electrolyte within a polymer electrolyte membrane (PEM): The effect of water and counterions. *Phys. Chem. Chem. Phys.* **2020**, *22*, 2917−2929.

(4) Kumar, A.; Hong, J.-W.; Yun, Y.; Bhardwaj, A.; Song, S.-J. The role of surface lattice defects of $CeO_2-\delta$ nanoparticles as a scavenging redox catalyst in polymer electrolyte membrane fuel cells. *J. Mater. Chem. A* **2020**, *8*, 26023−26034.

(5) Carton, J. G.; Olabi, A. G. Representative model and flow characteristics of open pore cellular foam and potential use in proton exchange membrane fuel cells. *Int. J. Hydrogen Energy* **2015**, *40*, 5726−5738.

(6) Li, Q.; He, R.; Jensen, J. O.; Bjerrum, N. J. PBI-based polymer membranes for high temperature fuel cells−preparation, characterization and fuel cell demonstration. *Fuel Cells* **2004**, *4*, 147−159.

(7) Wilberforce, T.; Alaswad, A.; Palumbo, A.; Dassisti, M.; Olabi, A. G. Advances in stationary and portable fuel cell applications. *Int. J. Hydrogen Energy* **2016**, *41*, 16509−16522.

(8) Lim, Y.; Lee, S.; Jang, H.; Hossain, M. A.; Gwak, G.; Ju, H.; Kim, D.; Kim, W. Sulfonated poly (ether sulfone) electrolytes structured with mesonaphthobifluorene graphene moiety for PEMFC. *Int. J. Hydrogen Energy* **2014**, *39*, 1532−1538.

(9) Rana, D.; Matsuura, T.; Zaidi, S. M. J. Research and development on polymeric membranes for fuel cells: an overview. *In: Polymer Membranes in Fuel Cells*, Zaidi, S. M. J.; Matsuura, T. (Eds.), Ch. 17, pp. 401−420, 2008, Springer Science Inc: New York, NY.

(10) Muthumeenal, A.; Sri Abirami Saraswathi, M.; Rana, D.; Nagendran, A. Recent research trends in polymer nanocomposite proton exchange membranes for electrochemical energy conversion and storage devices. *In: Membrane Technology: Sustainable Solutions in Water, Health, Energy and Environmental Sectors*, Sridhar, S. (Ed.), Ch 17, pp. 351−374, 2018, Taylor & Francis / CRC Press: Boca Raton, FL.

(11) Banerjee, J.; Dutta, K.; Rana, D. Carbon nanomaterials in renewable energy production and storage applications. *In: Emerging Nanostructured Materials for Energy and Environmental Science*, Rajendran, S.; Naushad, M.; Raju, K.; Boukherroub, R. (Eds.), Ch 2, pp. 51−104, 2019, Springer Nature: Switzerland., DOI: 10.1007/978-3-030-04474-9_2

(12) Divya, K.; Sri Abirami Saraswathi, M.; Rana, D.; Nagendran, A. Non-Nafion-based cation exchange membranes for direct methanol fuel cells. *In: Direct Methanol Fuel Cell Technology*, Dutta, K. (Ed.), Ch 3, pp. 37−70, 2020, Elsevier: Amsterdam, Netherlands.

(13) Şengül, E.; Erdener, H.; Akay, R. G.; Yücel, H.; Bac, N.; Eroğlu, İ. Effects of sulfonated polyether-etherketone (SPEEK) and composite membranes on the proton exchange membrane fuel cell (PEMFC) performance. *Int. J. Hydrogen Energy* **2009**, *34*, 4645−4652.

(14) Wong, C. Y.; Wong, W. Y.; Loh, K. S.; Daud, W. R. W.; Lim, K. L.; Khalid, M.; Walvekar, R. Development of poly (vinyl alcohol)-based polymers as proton exchange membranes and challenges in fuel cell application: a review. *Polym. Rev.* **2020**, *60*, 171−202.

(15) Kausar, A. Progression from polyimide to polyimide composite in proton-exchange membrane fuel cell: a review. *Polym.-Plast. Technol. Eng.* **2017**, *56*, 1375−1390.

(16) Escorihuela, J.; Olvera-Mancilla, J.; Alexandrova, L.; Del Castillo, L. F.; Compañ, V. Recent progress in the development of composite membranes based on polybenzimidazole for high temperature proton exchange membrane (PEM) fuel cell applications. *Polymer* **2020**, *12*, 1861.

(17) Li, Z.; Yao, Y.; Wang, D.; Hasan, M. M.; Suwansoontorn, A.; Li, H.; Du, G.; Liu, Z.; Nagao, Y. Simple and universal synthesis of sulfonated porous organic polymers with high proton conductivity. *Mater. Chem. Front.* **2020**, *4*, 2339−2345.

(18) Khanna, A. S. *Natural Degradation on Plastics and Corrosion of Plastics in Industrial Environment*. 2022: 956−986.

(19) McKeen, L.W. *Fluorinated coatings and finishes handbook: The definitive user's guide*. William Andrew 2015.

(20) Wang, L.; Deng, N.; Wang, G.; Ju, J.; Cheng, B.; Kang, W. Constructing amino-functionalized flower-like metal−organic framework nanofibers in sulfonated poly (ether sulfone) proton exchange membrane for simultaneously enhancing interface compatibility and proton conduction. *ACS Appl. Mater. Interfaces* **2019**, *11*, 39979−39990.

(21) Lu, D.; Zou, H.; Guan, R.; Dai, H.; Lu, L. Sulfonation of polyethersulfone by chlorosulfonic acid. *Polym. Bull.* **2005**, *54*, 21−28.

(22) Bekhoukh, A.; Moulefera, I.; Sabantina, L.; Benyoucef, A. Development, investigation, and comparative study of the effects of various metal oxides on optical electrochemical properties using a doped PANI matrix. *Polymer* **2021**, *13*, 3344.

(23) Mahmood, N.; De Castro, I. A.; Pramoda, K.; Khoshmanesh, K.; Bhargava, S. K.; Kalantar-Zadeh, K. Atomically thin two-dimensional metal oxide nanosheets and their heterostructures for energy storage. *Energy Storage Mater.* **2019**, *16*, 455−480.

(24) Díaz-Duran, A. K.; Roncaroli, F. MOF derived mesoporous nitrogen doped carbons with high activity towards oxygen reduction. *Electrochim. Acta* **2017**, *251*, 638−650.
(25) Rana, D.; Bag, K.; Bhattacharyya, S. N.; Mandal, B. M. Miscibility of Poly(styrene-co-butyl acrylate) with Poly(ethyl methacrylate): Existence of Both UCST and LCST. *J. Polym. Sci. Polym. Phys. Ed.* **2000**, *38*, 369−375.
(26) Rana, D.; Mandal, B. M.; Bhattacharyya, S. N. Analogue calorimetry of polymer blends: poly(styrene-co-acrylonitrile) and poly(phenyl acrylate) or poly(vinyl benzoate). *Polymer* **1996**, *37*, 2439−2443.
(27) Rana, D.; Mandal, B. M.; Bhattacharyya, S. N. Miscibility and phase diagrams of poly (phenyl acrylate) and poly (styrene-coacrylonitrile) blends. *Polymer* **1993**, *34*, 1454−1459.
(28) Luo, H.-B.; Ren, Q.; Wang, P.; et al. High proton conductivity achieved by encapsulation of imidazole molecules into proton-conducting MOF-808. *ACS Appl. Mater. Interfaces* **2019**, *11*, 9164−9171.
(29) Cai, Y. Y.; Yang, Q.; Zhu, Z. Y.; Sun, Q. H.; Zhu, A. M.; Zhang, Q. G.; Liu, Q. L. Achieving efficient proton conduction in a MOF-based proton exchange membrane through an encapsulation strategy. *J. Membr. Sci.* **2019**, *590*, No. 117277.
(30) Chuhadiya, S.; Suthar, D.; Patel, S. L.; Dhaka, M. S. Metal organic frameworks as hybrid porous materials for energy storage and conversion devices: A review. *Coord. Chem. Rev.* **2021**, *446*, No. 214115.
(31) Praveen, T.; Siva, M.; Berlina, M.; Dinakaran, K.; Paradesi, D. High Performance Bismuth Oxide Embedded Sulfonated Poly Ether Sulfone Composite Membranes for Fuel Cell Applications. *J. Macromol. Sci., Part A* **2023**, *60*, 171−180.
(32) Kim, M. K.; Kim, M. S.; Park, J. H.; Kim, J.; Ahn, C. Y.; Jin, A.; Mun, J.; Sung, Y. E. Bi-MOF derived micro/meso-porous Bi@ C nanoplates for high performance lithium-ion batteries. *Nanoscale* **2020**, *12*, 15214−15221.
(33) Gupta, G.; Umar, A.; Kaur, A.; Sood, S.; Dhir, A.; Kansal, S. K. Solar light driven photocatalytic degradation of Ofloxacin based on ultra-thin bismuth molybdenum oxide nanosheets. *Mater. Res. Bull.* **2018**, *99*, 359−366.
(34) Fan, X.; Zhang, A.; Li, M.; Xu, H.; Xue, J.; Ye, F.; Cheng, L. A reduced graphene oxide/bi-MOF-derived carbon composite as high-performance microwave absorber with tunable dielectric properties. *J. Mater. Sci.: Mater. Electron.* **2020**, *31*, 11774−11783.
(35) Zhang, L.; Ghimire, P.; Phuriragpitikhon, J.; Jiang, B.; Gonçalves, A. A.; Jaroniec, M. Facile formation of metallic bismuth/bismuth oxide heterojunction on porous carbon with enhanced photocatalytic activity. *J. Colloid Interface Sci.* **2018**, *513*, 82−91.
(36) Maria Mahimai, B.; Kulasekaran, P.; Deivanayagam, P. Novel polysulfone/sulfonated polyaniline/niobium pentoxide polymer blend nanocomposite membranes for fuel cell applications. *J. Appl. Polym. Sci.* **2021**, *138*, 51207.
(37) Di Vona, M. L.; Sgreccia, E.; Tamilvanan, M.; Khadhraoui, M.; Chassigneux, C.; Knauth, P. High ionic exchange capacity polyphenylsulfone (SPPSU) and polyethersulfone (SPES) cross-linked by annealing treatment: Thermal stability, hydration level and mechanical properties. *J. Membr. Sci.* **2010**, *354*, 134−141.
(38) Zakaria, Z.; Shaari, N.; Kamarudin, S. K. Preliminary study of alkaline direct ethanol fuel cell by using crosslinked Quaternized poly (vinyl alcohol)/graphene oxide membrane (Kajian Awal Sel Fuel Etanol Langsung Beralkali Menggunakan Membran Elektrolit Berasaskan Alkohol Polivinil Terkuaternisas). *J. Kejuruter.* **2018**, *30*, 219−227.
(39) Kang, S.; Pawar, R. C.; Pyo, Y.; Khare, V.; Lee, C. S. Size-controlled BiOCl−RGO composites having enhanced photodegradative properties. *J. Exp. Nanosci.* **2016**, *11*, 259−275.
(40) Wu, H.; Lian, K. The development of pseudocapacitive molybdenum oxynitride electrodes for supercapacitors. *ECS Trans.* **2014**, *58*, 25.
(41) Mingliang, L. U. O.; Qingzhi, W. E. N.; Jialin, L. I. U.; Hongjian, L. I. U.; Zilong, J. I. A. Fabrication of SPES/nano-TiO2 composite ultrafiltration membrane and its anti-fouling mechanism. *Chin. J. Chem. Eng.* **2011**, *19*, 45−51.
(42) Wang, G.; Liu, Y.; Huang, B.; Qin, X.; Zhang, X.; Dai, Y. A novel metal−organic framework based on bismuth and trimesic acid: synthesis, structure and properties. *Dalton Trans.* **2015**, *44*, 16238−16241.
(43) Liu, B.; Robertson, G. P.; Kim, D. S.; Sun, X.; Jiang, Z.; Guiver, M. D. Enhanced thermo-oxidative stability of sulfophenylated poly (ether sulfone) s. *Polymer* **2010**, *51*, 403−413.
(44) Gahlot, S.; Yadav, V.; Sharma, P. P.; Kulshrestha, V. Zn-MOF@ SPES composite membranes: synthesis, characterization and its electrochemical performance. *Sep. Sci. Technol.* **2019**, *54*, 377−385.
(45) Wen, S.; Gong, C.; Tsen, W. C.; Shu, Y. C.; Tsai, F. C. Sulfonated poly (ether sulfone)(SPES)/boron phosphate (BPO4) composite membranes for high-temperature proton-exchange membrane fuel cells. *Int. J. Hydrogen Energy* **2009**, *34*, 8982−8991.
(46) Hadis, Z.; Drew, H.; Yu, J.; Zhongwei, C.; Michael, F. Functionalized graphene oxide nanocomposite membrane for low humidity and high temperature proton exchange membrane fuel cells. *J. Phys. Chem. C* **2011**, *115*, 20774−20781.
(47) Deivanayagam, P.; Sivasubramanian, G.; Hariharasubramanian, K.; Baskar, B.; Gurusamy Thangavelu, S. A. Energy material-the role of silicotungstic acid and fly ash in sulfonated poly (ether sulfone) composites for PEMFC applications. *J. Macromol. Sci., Part A* **2019**, *56*, 146−152.
(48) Elakkiya, S.; Arthanareeswaran, G.; Venkatesh, K.; Kweon, J. Enhancement of fuel cell properties in polyethersulfone and sulfonated poly (ether ether ketone) membranes using metal oxide nanoparticles for proton exchange membrane fuel cell. *Int. J. Hydrogen Energy* **2018**, *43*, 21750−21759.

https://doi.org/10.1021/acsomega.3c03143
ACS Omega 2023, 8, 27510−27518